JAEHR
Journal of Advances in Environmental Health Research
J Adv Environ Health Res. 2025;13(2):104-113. doi: 10.34172/jaehr.1373
http://jaehr.muk.ac.ir

Original Article

Hydrogeochemical Characterization Using Piper Diagram of the Groundwater Surrounding the Wild Dump of the El Hajeb Town, Morocco

Abderrahmane Gamar[1*], **Zakaria Khiya**[1]

[1]Department of Chemistry, Faculty of Science, University Moulay Ismail, Meknes, Morocco

Article history:
Received: January 24, 2024
Revised: June 5, 2024
Accepted: July 6, 2024
ePublished: April 20, 2025

***Corresponding author:**
Abderrahmane Gamar,
Email: abdergama@gmail.com

Abstract

Background: The availability of groundwater with acceptable quality has become a significant challenge in many regions worldwide, particularly in Morocco. This issue is exacerbated by severe climatic conditions and pollution, which render groundwater resources increasingly vulnerable to various contamination factors. The Plateau of the El Hajeb region is part of the Causse Middle Atlas and the water table of the grand basin of Saïs, two major main reservoirs of groundwater in Morocco. In this context, the primary aim of this study is to identify the geochemical facies of the groundwater in the region housing the municipal waste dump. Additionally, the study seeks to determine the sources of mineralization affecting these waters.

Methods: Over the course of two sampling campaigns conducted between 2015 and 2018, groundwater samples were collected from 97 points. These points were strategically located around the municipal waste dump and along the groundwater flow, including wells, boreholes, and springs. Analyses were conducted in accredited laboratories following standardized methods, with a focus on the determination of major ions.

Results: The results of the geochemical analysis, as represented by the Piper diagram, revealed a calco-bicarbonate facies with low mineralization. This low mineralization does not affect the potability of the waters, thus maintaining their suitability for human consumption. The carbonate formations (calcite and dolomite) constitute the host rocks of the groundwater.

Conclusion: Chlorination and/or sulfation alteration processes were observed, contributing to the presence of specific ionic species associated with anthropogenic pollution.

Keywords: Groundwater, Analyzes, Geochemical facies, Piper's diagram, Morocco

Please cite this article as follows: Gamar A, Khiya Z. Hydrogeochemical characterization using piper diagram of the groundwater surrounding the wild dump of the El Hajeb town, Morocco. J Adv Environ Health Res. 2025; 13(2):104-113. doi:10.34172/jaehr.1373

Introduction

The Atlas domain serves as the structural backbone of Morocco, stretching from the northeast to the southwest between latitudes 31°N and 34°N.[1,2] It forms a significant high-altitude mountain barrier, dividing the country into two distinct climatic regions: the northwest, influenced by oceanic effects, and the southeast, characterized by an arid Saharan climate.[3,4]

The central and northeastern regions of the Atlas domain are characterized by a substantial limestone series, coupled with extensive and prolonged snow cover across much of the mountain range. These features establish the Atlas as a significant "water tower," supplying water resources to approximately four-fifths of Morocco's land area.[5-9]

Population growth in the region, combined with intensive agriculture, industrial development, and recurrent droughts, poses significant challenges to groundwater management. These factors compromise the ability to ensure a sustainable supply of groundwater, both in terms of quantity and quality, for the surrounding towns and villages over time.[10-15] The combined effect of drought and overexploitation of the Causses aquifer results in an annual destocking of the aquifer reserves by 10 Mm^3. This destocking will have negative impacts on surface and underground water resources since the Causses area represents the water tower ensuring more than 50% of the supply of the Saïs aquifer system.[12]

The Middle Atlas Causses aquifer, situated between the Fez-Meknes basin to the north and the Middle Atlas to the south, spans an area of approximately 4600 km^2. This aquifer is composed of tabular carbonate formations from the Lias period. However, its geometry and hydrogeological characteristics remain poorly understood. The water quality in this aquifer is notably high, with a mineralization level of less than 0.5 g/L.[1,16]

The recharge of the water table occurs exclusively through

rainwater infiltration. This resource is extracted primarily via boreholes and wells for irrigation purposes.[17,18]

In the Saïs Basin (Figure 1), the Liassic and Miocene formations overlie the Triassic clays, basalts, and evaporites and are, in turn, overlain by Pliocene-Quaternary limestone and travertine.[19] These carbonates are affected by several fractures causing a dislocation of different Liassic blocs and sometimes Pliocene-Quaternary limestone-travertine.[20,21] The groundwater flows in this region are conditioned by two major fracture networks, mainly NE–SW and NW–SE directions,[12,20,22] and probably with a NW–SE preferential flow direction.[23]

Materials and Methods

Study Area

The Plateau of the El Hajeb region (Figure 1) forms part of the Tabular Middle Atlas. It hosts a groundwater table that circulates within Liassic limestone and dolomite formations, providing substantial water quantities and representing significant hydrological potential.[1,19,20,24] The Liassic carbonates dip northward at the junction of the Tabular Middle Atlas and the Saïs Basin, beneath a thick deposit of Miocene marls, thereby forming a confined aquifer.[16]

At the junction of the El Hajeb Plateau and the Saïs Basin (Figure 1), several karst springs serve as outlets, draining travertine deposits.[19] The confined aquifer is characterized by emergences and overflow springs along the edge of the Causse, flexure springs, and hydrothermal springs in the Saïs region.[25]

The confined aquifer flows primarily through the carbonate formations of the Lias but occasionally also through molasse deposits, consisting of sandstone, sands, and conglomerates, located at the base of the transgressive Miocene, which overlies the Lias.[12,26-29] A karstic complex water circulation is especially developed locally at the border of the two hydrogeological units.[30]

The study area (Figure 2) is underlain by a significant aquifer reservoir, specifically the deep aquifer, which is unconfined at the level of the Causse but becomes confined beneath the impermeable Tertiary deposits. This aquifer is recharged through the infiltration of rain and snow from the Middle Atlas Causse.[20,31] It is also recognized and exploited through boreholes, which, in the northern part, are artesian and highly productive.[32-35]

The deep and shallow aquifers of the Saïs Basin are replenished by rainfall, water from the Tabular Middle Atlas, and springs located along the boundary between the Tabular Middle Atlas and the Saïs Basin. These represent the most important water supply of the region for drinking and agricultural uses.[36-38] However, the modalities of water transfer between the Middle Atlas Causses and Saïs basin and the interactions of water with the different geological facies are not well known.[16]

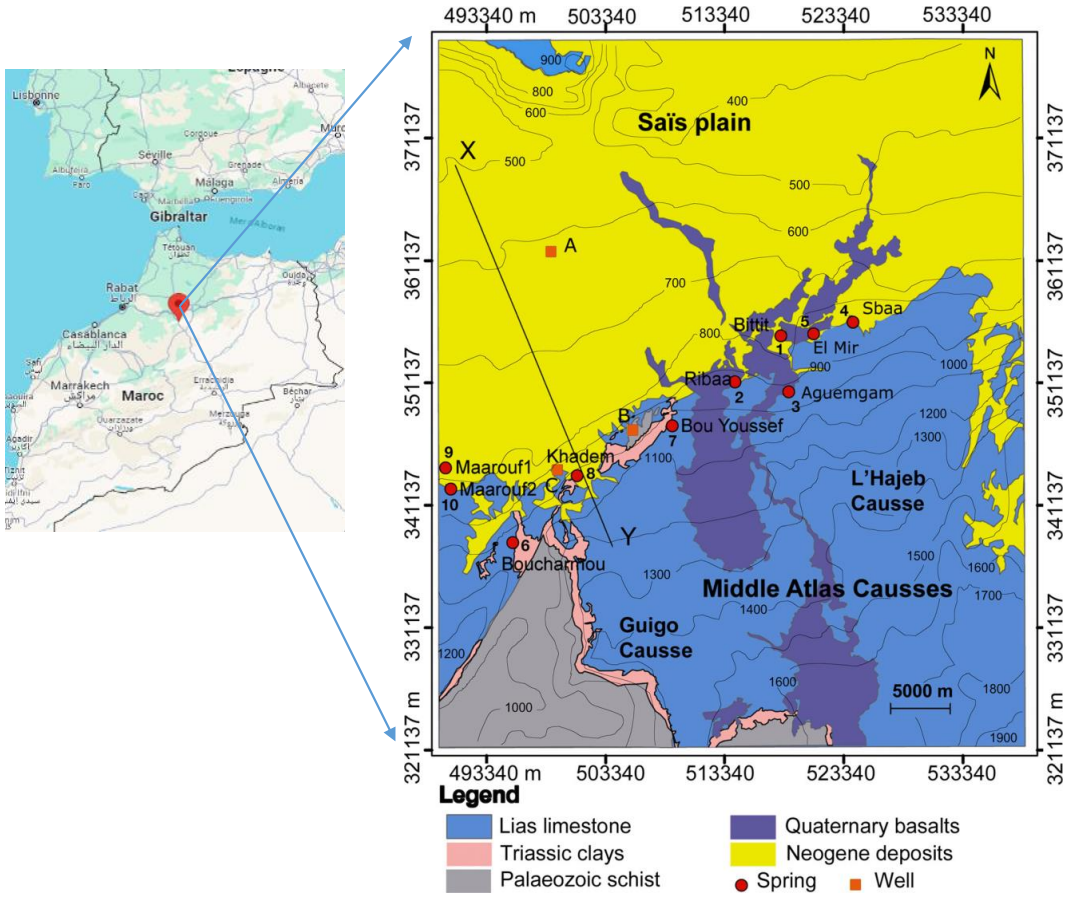

Figure 1. Geological Section of the Study Area According to the Geological Map of El Hajeb

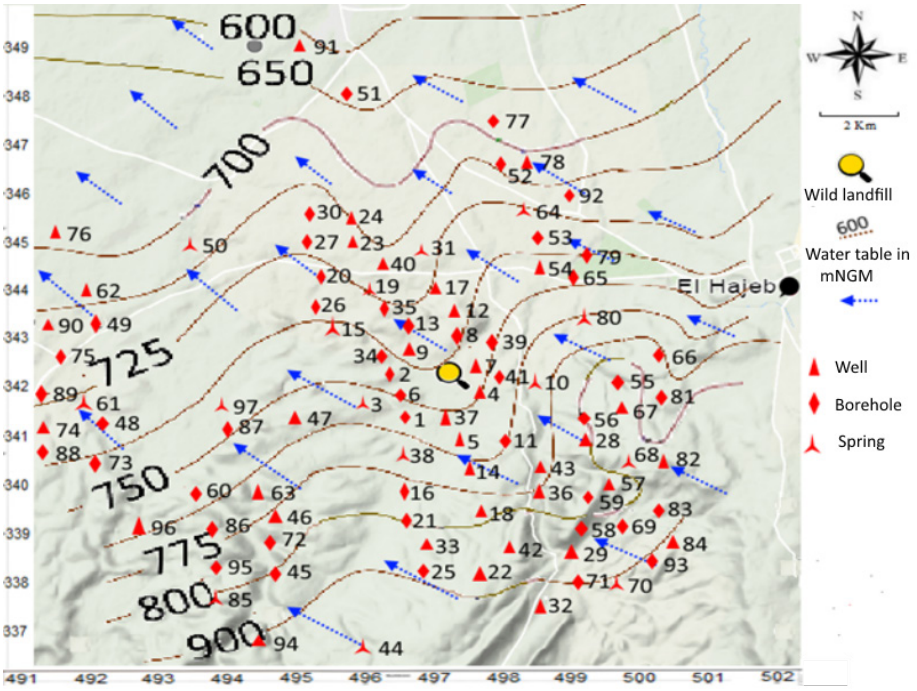

Figure 2. Piezometric Map Showing the Positioning of Wells, Sources and Boreholes

The purpose of this study is to characterize the aquifer of the El Hajeb region (Morocco) from a hydro-geochemical point of view, to explain outcomes and dynamics of the changes of ions and cations concentrations, and to find the mineralization origin of host of these water resources by exploiting the modeling of PHREEQC (version 2.7).[39]

Sampling and Laboratory Analyses

The diverse climatic conditions, hydrological regimes, and geological environments of this region result in a wide variety of groundwater types. To characterize the facies of these waters, two sampling campaigns were conducted at 97 stations, represented by W (wells), B (boreholes), and S (springs). The sampling sites were distributed across the entire study area, with higher density near the waste dump and along the groundwater flow direction, particularly at the junction between the Saïs Plain and the Tabular Middle Atlas, following the NE–SW orientation (Figure 2).

The first sampling campaign lasted two years, from May 2015 to January 2017, while the second campaign lasted one year, from February 2017 to January 2018. The locations of the water points were determined using a Garmin-type GPS, and the static water levels were measured with a piezometric probe. A technical sheet was prepared, indicating the distances of the 97 sampling stations from the waste dump, as well as their depths (Table 1). Water samples were collected in polyethylene bottles, previously washed with an alkaline solution and rinsed with double-distilled water, and then transported to the laboratory at 4°C.

Physico-chemical variables, including temperature, pH, electrical conductivity, and dissolved oxygen, were measured on-site using portable devices. The geochemical characterization of major elements was performed as follows: chlorides (Cl^-) by the Mohr method, sulfates (SO_4^{2-}) by turbidimetry, nitrates (NO_3^-) by visible spectrophotometry with adsorption on a column, and bicarbonates (HCO_3^-) by volumetric analysis. Calcium (Ca^{2+}) and magnesium (Mg^{2+}) were analyzed using atomic absorption spectroscopy, while sodium (Na^+) and potassium (K^+) ions were measured by flame spectrophotometry (Horiba Jobin-Yvon ICP-OES).

Tools and methods

To effectively analyze this data and extract the maximum amount of information within a limited timeframe, it was essential to apply efficient and rapid tools and methods. The primary tool used for this purpose is DIAGRAMMES software, developed by Roland Simler of the Avignon Hydrogeology Laboratory.[40] This free, open-source software is specifically designed for hydrochemical analysis, facilitating water quality assessments. One of its key functions is the generation of Piper diagrams, which visually represent the distribution of anions and cations across two specific triangles. These triangles depict the relative concentrations of major ions in comparison to the total concentration of these ions—cations are represented in the left triangle, while anions are represented in the right triangle. The relative position of a sample's analytical result within each triangle allows for the identification of the dominant anion and cation species. Additionally, these two triangles are linked to a rhombus, where the intersection of lines drawn from the points on each triangle is plotted. The point of intersection within the rhombus provides a global analysis of the water sample, with its location helping to identify the specific facies of the studied water.

Table 1. Technical Data Sheet of the Sampling Stations Indicating Their Coding, Depths and Distances From the Wild Dump

Station Coding	Depth (m)	Distance From the Landfill (m)
B1	15.5	462.13
B2	13.5	512.66
S3	-	635.20
W4	17.5	306.63
W5	15	407
B6	17	302.82
W7	16	356.19
B8	14.5	429.77
W9	16.5	466.63
S10	-	508
B11	21.5	461
W12	19.5	1262
B13	18.5	1296
W14	20	608
S15	-	1579
B16	26.5	915
W17	20.5	1491
W18	29	1314
S19	-	1761
B20	23	1822
B21	31	1310
W22	14	1971
W23	24.5	1854
W24	17	1907
B25	30.5	1624
B26	31	1810
B27	30	1939
W28	26	1310
W29	15	2042
B30	27.5	1974
S31	-	1665
W32	28.5	2152
W33	13.5	1480
B34	24	1417
B35	28	1501
W36	23	1308
W37	15	358.06
S38	-	499
B39	31	504.40
W40	15.5	1704
B41	30.5	400.25
W42	18	1708
W43	19	1131
S44	-	4190
B45	13.5	5370
W46	-	5144
W47	17.5	2988
B48	15	5455

Table 1. Continued.

Station Coding	Depth (m)	Distance From the Landfill (m)
B49	17	4987
S50	-	2694
B51	14.5	2479
B52	16.5	2305
B53	18	2388
W54	21.5	2177
B55	19.5	1905
B56	18.5	1615
W57	20	1838
B58	-	1711
B59	26.5	1723
B60	20.5	7085
S61	-	5918
W62	30	6219
W63	23	5410
S64	-	2407
B65	14	1972
B66	24.5	2246
W67	17	1849
S68	-	1874
B69	31	2009
S70	-	2401
B71	26	2041
B72	15	4045
B73	27.5	6346
W74	-	6529
B75	28.5	5840
W76	13.5	6147
B77	24	2830
W78	28	2491
B79	23	2292
S80	-	2035
B81	17,5	2134
W82	31	2177
B83	15.5	2336
W84	30.5	2565
S85	-	6800
B86	19	7197
B87	28.5	4666
B88	13.5	6834
B89	24	6636
W90	28	6395
W91	23	3166
B92	28.5	2636
B93	13.5	2428
W94	24	5347
B95	28	6575
W96	23	6871
S97	-	4002

Results and Discussion

Physico-chemical Quality of Groundwater

The analysis of the physicochemical quality of groundwater reveals variations in concentration across the different measurement points (Table 2).

Table 2. Physico-chemical Quality of Groundwater

Parameters	Mean ± SE	Min	Max
T	19.22 ± 0.31	12.2	23.2
pH	7.22 ± 0.05	6.13	8.15
EC	899.47 ± 73.72	310.65	3710.35
Turb	9.34 ± 0.54	1.41	19.57
Eh	489.15 ± 24,32	72.92	777.34
TDS	587.31 ± 158,97	74.23	13781.9
Sal	342.33 ± 31,51	20.45	1090.47
TSS	108.51 ± 9.45	1.38	295.42
Cl	129.63 ± 11.24	8.19	386.76
CAT	9.45 ± 0.42	5.47	18.47
TH	41.92 ± 1.74	15.12	77.75
BOD5	2.42 ± 0.1	1.01	4.98
PI	4.44 ± 0.23	1.11	8.21
Na	308.30 ± 41.4	113.13	1336.42
SO4	37.92 ± 5.65	0.09	217.45
NH4	0.29 ± 0.03	0.01	1.47
PO4	0.16 ± 0.02	0.001	1.15
SiO2	10.24 ± 0.63	1.43	21.45
HCO3	398.21 ± 9.93	232.37	557.51
SO4	37.92 ± 5.65	0.09	217.45
F	0.36 ± 0.06	0.002	2.17
NO3	63.93 ± 3.22	0.33	96.25
NO2	0.19 ± 0.03	0.001	0.99
TH	41.92 ± 1.74	15.12	77.75
I	0.38 ± 0.05	0.00	1.78
DO	6.33 ± 0.17	2.37	8.62

All parameters are expressed in mg/L except pH without unit; T in °C; EC in µS/Cm; CAT and TH in °F; Min: Minimal value; Max: Maximal value; Mean: Average value; SE: Standard Error; PI: Oxidizability; DO: Dissolved O2.

Study of Facies: Piper Diagram

The representation of the samples on the Piper diagram (Figure 3) revealed the presence of dominant chemical facies, with their distribution being influenced by the lithology of the soil in which the aquifer was situated throughout the observation period. The identified facies are as follows:

- *Calcium bicarbonate facies,* which accounted for 77% of the stations (S3, W12, B13, W14, S15, B16, W17, W18, S19, W22, W23, W24, B25, B27, W29, B30, W32, W36, B39, W42, W46, S50, B53, W54, B56, S61, W63, S64, B73, W74, S80, W82, B87);
- *Chlorinated-calcium facies,* which were observed at only 2% of the surveyed stations (W37 and B60);
- *Chloride-sodium facies,* represented by 15% of the stations (B1, B2, W4, B6, W7, B8, W9, B20, B34, S38, W40, B41, B55);
- *Bicarbonate-sodium facies,* which were found at 6% of the stations (S10, W17, W23, B27, B30, S31, B35, S50, B51, B53, B73, B87, B88).

The calcium carbonate facies is the dominant facies, reflecting the influence of the dissolution of gypsum ($CaSO_4$) and halite (NaCl) present in the limestones and dolomites of the Middle Atlas on the chemical composition of the waters. This explains the high concentrations of bicarbonates and calcium. This facies is observed upstream of the waste disposal site, where it originates from the carbonate formations bordering the aquifer. The

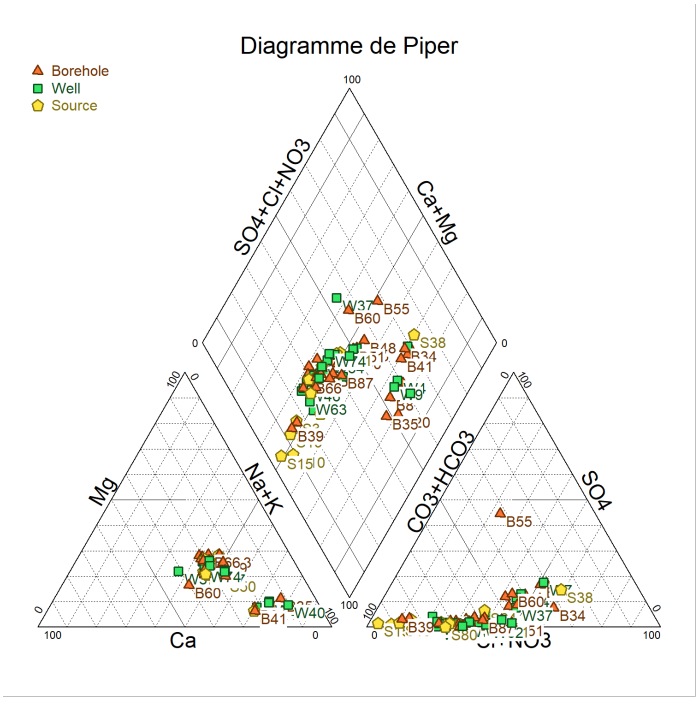

Figure 3. Piper Diagram of Wells, Springs and Boreholes in the El Hajeb Region

results are consistent with the study by Miche et al[16] on the spring waters at Khadem, Maarouf 1, and Maarouf 2 sites, which are part of the present study area. Furthermore, the findings align with a similar study by Nour et al,[41] which demonstrated that the distribution of cations and anions in the Piper diagram indicated a dominant facies of calcium and magnesium bicarbonates, comprising 75% of the groundwater samples from the town of Gagal in southwestern Chad. The chlorinated facies can be attributed, in addition to the lithological characteristics of the soil, to the proximity of sampling stations to the waste disposal site, which generates leachates. However, the exceptions are boreholes B55 and B60, which are located farther from the landfill and are likely influenced by septic tanks and latrines, which contribute wastewater. This chlorinated facies is also present in the Piper diagram in the study by Miche et al,[16] although the origin of the facies was not further discussed.

Na^+/Cl^- Report

The Na/Cl ratio provides insight into the origin of chloride contamination. A molar Na/Cl ratio of less than 0.86 typically indicates water that has been impacted by pollution.[42] Na and K, being alkaline metals, are commonly found in natural environments. In uncontaminated groundwater, their concentrations rarely exceed 100 mg/L for Na and 90 mg/L for K. The Na/K ratio in weakly mineralized water typically ranges from 0.2 to 0.9; this ratio tends to increase with rising mineralization, often reaching values between 30 and 200.[43]

This study serves as a valuable tool for tracing the origin of mineralization.[44] Na behaves as a function of chloride content, with chloride being considered a conservative ion. It is highly soluble, rarely involved in chloride salt precipitation, not affected by redox processes, and unaffected by bacterial activity.[45] Figures 4 and 5 reveal five distinct groups:

The first group consists primarily of stations exhibiting a strong correlation between the Cl/Na ratio and chloride concentration (Figure 4). It can be deduced that the Na concentration varies slightly, a finding supported by Figure 4.

The second group shows a Cl/Na ratio of 0.18. The third group presents a Cl/Na ratio of 0.2. The fourth group has a Cl/Na ratio of 0.3. These last three groups display an enrichment of Na accompanied by a reduction in chloride, with chloride concentrations decreasing from the second to the fourth group. The fifth group contains only one station, W37, where the Cl/Na ratio is 1.1 (greater than 1), indicating an enrichment in chloride and a Na deficit (Figures 4 and 5). This is likely attributable to anthropogenic pollution.

The results of the first four groups of water align closely with findings from the Tertiary aquifers and the base of the supply zone (BR02), the Ypresian aquifer (hill region) (BR04), and the Bruxellian aquifer (BR05) in the Brussels-Capital Region, as reported by Thomas et al[46] Their study revealed that some points exhibited Na/Cl ratios greater than 0.86, likely reflecting Na enrichment due to Na-Ca cationic exchanges during cooling processes. In this phenomenon, Na ions adsorbed onto geological material in the subsurface are released into the water, displacing calcium ions, which take their place on the adsorption sites.

The results for the fifth group are also consistent with the study by Thomas et al[46] They noted that certain points had Na/Cl ratios lower than that of seawater (0.86). This suggests that, for these points, the source of chloride was not ancient marine water or halite dissolution but likely of anthropogenic origin, such as pollution.

Ca^{2+}/Mg^{2+} Ratio

A priori, the evaporitic origin of magnesium is weak and comes

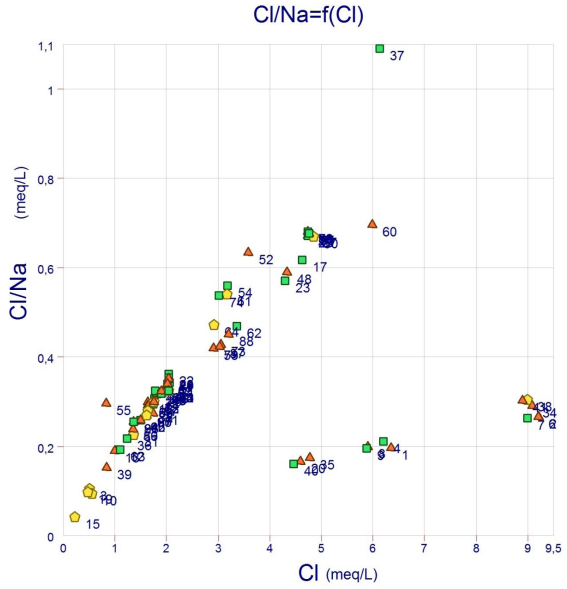

Figure 4. Relationship between Cl/Na and Cl

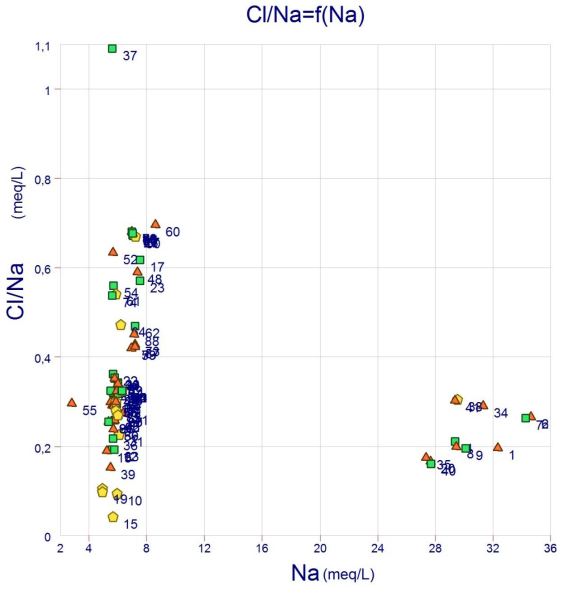

Figure 5. Relationship Between Cl/Na and Na

from the dissolution of dolomites, dolomitic limestones, and ferromagnesian minerals. Calcium comes from the dissolution of calcite ($CaCO_3$) and gypsum ($CaSO_4$), which are easily soluble. Magnesium is an element that often accompanies calcium. At first glance, Figure 6 illustrates a relatively strong correlation between the Ca/Mg ratio and calcium content, suggesting that the magnesium (Mg) levels remain relatively constant across these stations. Furthermore, the Ca/Mg ratio allows for the distinction of two groups: the first group, with a Ca/Mg ratio of less than 1, indicates that magnesium predominates over calcium. The second group, comprising the majority of the stations, has a Ca/Mg ratio greater than 1, suggesting that calcium predominates over magnesium (Figures 6 and 7). These results align closely with the findings of Miche et al,[16] as previously mentioned. Their study reported a higher Mg/Ca ratio (1.1) in certain springs of Type I in the western sector of the El Hajeb region. This was likely due to advanced dolomite dissolution followed by calcite precipitation in an aquifer with longer water transit times. Another possible explanation for the elevated Mg/Ca ratio could be the hydrolysis of magnesium-rich silicates in Quaternary and Triassic basalts. It is worth noting that the causses in the study area were formed during the same period and share a similar geological composition, primarily consisting of dolomite and calcite. From a geochemical perspective, dolomite, which is difficult to reprecipitate,[47] exhibits a notable distinction between the eastern and western regions. In the western part of the study area, the longer transit times favor the reprecipitation of calcite, resulting in a higher Mg/Ca ratio in the Lias aquifer.

Na^+/K^+ Ratio

The presence of Na in water can be anthropogenic or naturally occurring in the soil.

Potassium is an alkaline metal with high reactivity in the presence of water. It predominantly occurred in igneous rocks and naturally exists as double chlorides in various mineral ores. Additionally, K was found in vegetation in the form of carbonate. Its primary sources include the alteration of silicate formations, such as gneiss and shale, the presence of K-rich clays, and the dissolution of nitrogen-phosphorus-potassium (NPK) fertilizers. The Na/K ratio is approximately 47 in seawater and less than 10 in rainwater.[48,49] In these waters, the present study classifies the various water brands from the sampled stations into four distinct groups based on Na enrichment (Figures 8 and 9). The first group, consisting of most stations with relatively lower Na content, exhibits an Na/K ratio ranging from 10 to 44. The second group, characterized by lower K content, has a ratio between 72 and 90. The third group, also K-deficient, presents ratios ranging from 105 to 115. Finally, the fourth group, with a Na-enriched composition, demonstrates ratios between 15 and 20. The findings for the first group are consistent with the results reported by Szymanska-Pulikowska,[50] who conducted a study from 1995 to 2007 on Na and K concentrations in groundwater near the Maślice municipal refuse dump in Wrocław. The study indicated that Na and K concentrations generally remained within natural ranges, except during the years 2000–2001. During the study period, the Na/K ratio ranged from 2.52 to 14.04.

HCO_3^-/Na^+ Ratio

The HCO_3/Na ratio can serve as an indicator for assessing weathering processes in groundwater.[51,52] A ratio greater than 1 suggests the predominance of carbonate weathering, whereas a ratio less than 1 indicates silicate weathering. Figure 10 illustrates the relationship between bicarbonate and Na ion concentrations, revealing three distinct groups. The first group exhibits a ratio of $0.6 < HCO_3/Na < 1$, with noticeable Na enrichment, suggesting that silicate weathering is the dominant process controlling groundwater chemistry. Similar findings were reported by

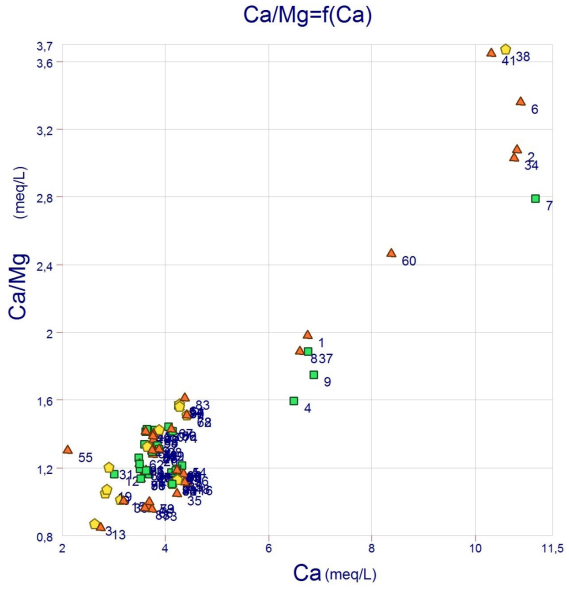

Figure 6. Relationship Between Ca/Mg and Ca

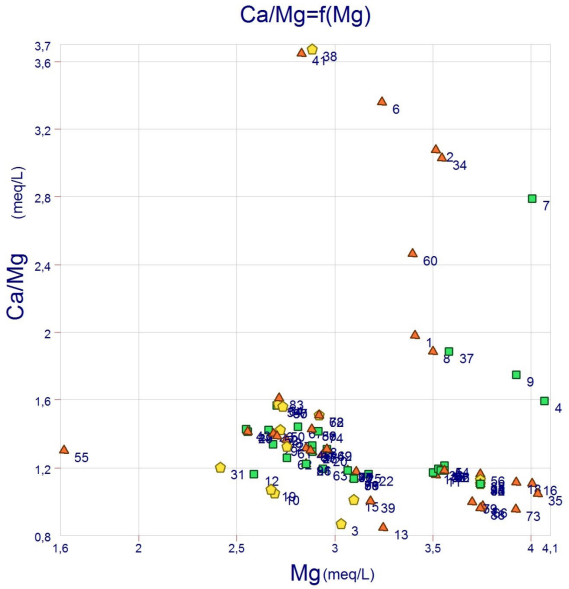

Figure 7. Relationship Between Ca/Mg and Mg

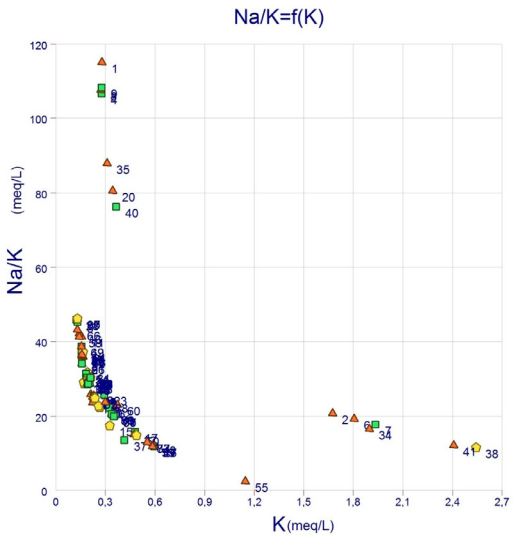

Figure 8. Relationship Between Na/K and K

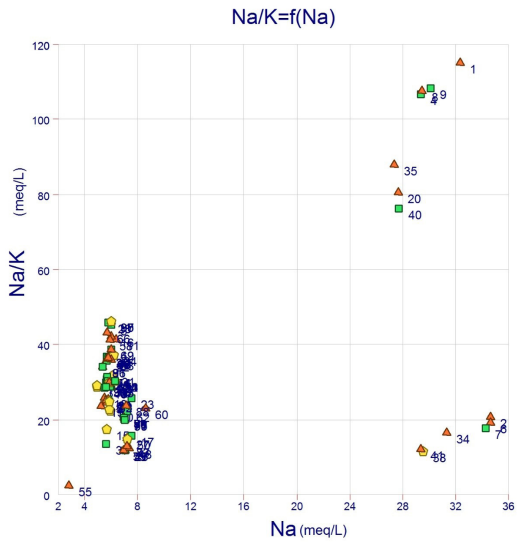

Figure 9. Relationship Between Na/K and Na

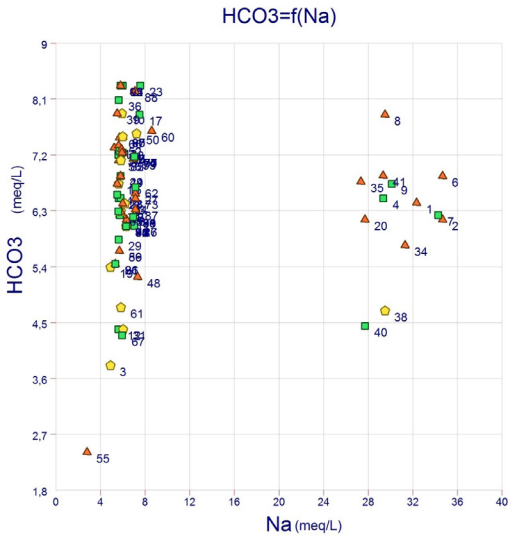

Figure 10. Relationship Between HCO_3 and Na

Matini et al.[53] in a study of groundwater from Brazzaville, Congo, where the HCO_3/Na ratio ranged from 66.66 to 33.34% for silicate and carbonate weathering, respectively, during the rainy season, and from 60.87 to 39.13% during the dry season.

The second group exhibits an HCO_3/Na ratio ranging from 1 to 1.42, indicating bicarbonate enrichment, while the third group is characterized by Na enrichment, with an HCO_3/Na ratio varying between 0.12 and 0.29. Bicarbonates are commonly present in natural waters, primarily resulting from the dissolution of carbonate formations such as limestone and dolomite. The behavior of water in this context depends on its equilibrium state. The presence of bicarbonates in groundwater can be attributed to the dissolution of carbonate rocks, such as cipolin and limestone, through interaction with carbon dioxide-enriched water. The overall dissolution process can be represented by the following equations[54,55]:

$$CaCO_{3(s)} + H_2O_{(l)} + CO_{2(g)} \rightarrow 2HCO_{3\,(aq)}^{-} + Ca^{2+}{}_{(aq)}$$

Conclusion

The groundwater in the El Hajeb region is primarily recharged through the infiltration of precipitation, including rain and snow, originating from the Middle Atlas mountain range. This recharge subsequently feeds the Saïs plain. Mineralization, occurring in an open system, results from the dissolution of the geological matrix and the interaction with biogenic CO_2. A hydrogeochemical analysis, conducted using the Piper diagram, revealed that these waters are predominantly of the calcium-bicarbonate facies. However, evidence of chlorinated and/or sulfated alteration processes indicates the presence of ionic species of anthropogenic origin.

The major ionic composition suggests that water-rock interactions are the principal processes governing the chemistry of the investigated groundwater. Most stations exhibit a carbonate-soda-lime mineralogical signature (HCO_3–Na–Ca), which does not significantly compromise the potability of the water. The concentrations of these ionic components vary, generally decreasing from upstream, near the Middle Atlas, to downstream in the Saïs plain, following the groundwater flow direction and associated precipitation phenomena. Additionally, the residence time of groundwater within the aquifer plays a crucial role in shaping the geochemical facies of these waters.

Acknowledgments

This study was conducted in cooperation with the National Laboratory of the Studies and the Monitoring of the Pollution of Rabat, Morocco and the National Office of Electricity and Drinking Water -drinking water branch of Meknes, Morocco. The author (s) would like to express their appreciation to those who helped us in this study.

Authors' Contribution

Conceptualization: Abderrahmane Gamar.

Data curation: Abderrahmane Gamar, Zakaria Khiya.
Formal analysis: Abderrahmane Gamar.
Funding acquisition: Abderrahmane Gamar, Zakaria Khiya.
Investigation: Abderrahmane Gamar.
Methodology: Abderrahmane Gamar.
Project administration: Abderrahmane Gamar, Zakaria Khiya.
Resources: Abderrahmane Gamar.
Resources: Abderrahmane Gamar.
Software: Abderrahmane Gamar.
Supervision: Abderrahmane Gamar.
Validation: Abderrahmane Gamara.
Visualization: Abderrahmane Gamar.
Writing–original draft: Abderrahmane Gamar.
Writing–review & editing: Abderrahmane Gamar.

Competing Interest

The authors declare that they have no conflict of interest.

Ethical Approval

This research was conducted in accordance with ethical guidelines, and no specific ethical considerations were applicable to this study.

Funding

This study was self-funded by the authors and received no external financial support from any funding organization.

References

1. Missenard Y, Zeyen H, Frizon de Lamotte D, Leturmy P, Petit C, Sébrier M, et al. Crustal versus asthenospheric origin of relief of the Atlas Mountains of Morocco. J Geophys Res Solid Earth. 2006;111(B3):B03401. doi: 10.1029/2005jb003708.
2. Ellero A, Ottria G, Malusà MG, Ouanaimi H. Structural geological analysis of the High Atlas (Morocco): evidences of a transpressional fold-thrust belt. In: Sharkov E, ed. Tectonics-Recent Advances. IntechOpen; 2012. doi: 10.5772/50071.
3. Weldeab S, Lea DW, Schneider RR, Andersen N. 155,000 years of West African monsoon and ocean thermal evolution. Science. 2007;316(5829):1303-7. doi: 10.1126/science.1140461.
4. Tjallingii R, Claussen M, Stuut JB, Fohlmeister J, Jahn A, Bickert T, et al. Coherent high- and low-latitude control of the northwest African hydrological balance. Nat Geosci. 2008;1(10):670-5. doi: 10.1038/ngeo289.
5. Charrière A. Héritage hercynien et évolution géodynamique alpine d'une chaine intracontinentale: le Moyen-Atlas au sud-est de Fes (Maroc) [dissertation]. Etat, Toulouse-III. 1990. p. 589.
6. Charroud M. Evolution géodynamique de la partie sud-ouest du Moyen Atlas durant le passage Jurassique Crétacé, le Crétacé et le Paléogène [dissertation]. Rabat: Université Mohammed V; 1990. p. 232.
7. Frizon de Lamotte D, Crespo-Blanc A, Saint-Bézar B, Comas M, Fernadez M, Zeyen H, et al. TRASNSMED-transect. In: Cavazza W, Roure F, Spakman W, Stampfli GM, Ziegler PA, eds. The TRANSMED Atlas — The Mediterranean Region from Crust to Mantle. Berlin: Springer; 2004. p. 91-6.
8. Frizon de Lamotte D, Zizi M, Missenard Y, Hafid M, Azzouzi ME, Maury RC, et al. The atlas system. In: Michard A, Saddiqi O, Chalouan A, de Lamotte DF, eds. Continental Evolution: The Geology of Morocco: Structure, Stratigraphy, and Tectonics of the Africa-Atlantic-Mediterranean Triple Junction. Berlin, Heidelberg: Springer; 2008. p. 133-202. doi: 10.1007/978-3-540-77076-3_4.
9. Sabaoui A. Rôles des inversions dans l'évolution mésocénozoïque du Moyen Atlas Septentrional (Maroc). [dissertation]. L'exemple de la transversale EL Menzel - Ribat al Khayr - Bou Iblane; 1998. p. 410.
10. Amraoui F, Razack M, Bouchaou L. Comportement d'une source karstique soumise à une sécheresse prolongée: la source Bittit (Maroc). Collect C R Geosci. 2004;336(12):1099-109. doi: 10.1016/j.crte.2004.03.016.
11. Bzioui M. Rapport national 2004 sur les ressources en eau au Maroc. UN Water Africa; 2004. p. 94.
12. Amraoui F. Contribution à la reconnaissance des aquifères karstiques, cas du Lias de la plaine de Saiss et du causse moyen atlasique tabulaire (Maroc) [dissertation]. Casablanca, Maroc: Université Hassan II Ain Chock, Faculté des Sciences; 2005. p. 227.
13. Luterbacher J, Xoplaki E, Casty C, Wanner H, Pauling A, Küttel M, et al. Mediterranean climate variability over the last centuries: a review. In: Lionello P, Malanotte-Rizzoli P, Boscolo R, eds. Developments in Earth and Environmental Sciences. Vol 4. Amsterdam: Elsevier; 2006. p. 27-148. doi: 10.1016/s1571-9197(06)80004-2.
14. Esper J, Büntgen U, Frank DC, Nievergelt D, Liebhold A. 1200 years of regular outbreaks in alpine insects. Proc R Soc Lond B Biol Sci. 2006;274(1610):671-9. doi: 10.1098/rspb.2006.0191.
15. Etebaai I, Damnati B, Raddad H, Benhardouz H, Benhardouz O, Miche H, et al. Impacts climatiques et anthropiques sur le fonctionnement hydrogéochimique du Lac Ifrah (Moyen Atlas marocain). Hydrol Sci J. 2012;57(3):547-61. doi: 10.1080/02626667.2012.660158.
16. Miche H, Saracco G, Mayer A, Qarqori K, Rouai M, Dekayir A, et al. Hydrochemical constraints between the karst Tabular Middle Atlas Causses and the Saïs basin (Morocco): implications of groundwater circulation. Hydrogeol J. 2018;26(1):71-87. doi: 10.1007/s10040-017-1675-0.
17. Bouchaou L, Tagma T, Boutaleb S, Hssaisoune M, El Morjani ZE. Climate change and its impacts on groundwater resources in Morocco: the case of the Souss-Massa basin. In: Climate Change Effects on Groundwater Resources: A Global Synthesis of Findings and Recommendations. CRC Press; 2011. p. 129-44.
18. Ait Kadi M, Ziyad A. Integrated water resources management in Morocco. In: Global Water Security: Lessons Learnt and Long-Term Implications. Singapore: Springer; 2018. p. 143-63. doi: 10.1007/978-981-10-7913-9_6.
19. Chamayou J, Combe M, Genetier B, Leclerc C. Le bassin de Meknès-Fè. In: Maroc EdS, Ed. Ressources en Eau du Maroc; 1975. p. 41-71.
20. Bentayeb A, Leclerc C. Le Causse moyen- atlasique. In: Editions du Service Géologique du Maroc, Ed. Ressources en Eau du Maroc; 1977. p. 37-84.
21. Martin J. Le Moyen Atlas central. Etude. Etude Géomorphologique. Notes et Mémoires du Service géologique du Maroc. No. 258 bis. 1981.
22. Essahlaoui A, Sahbi H, Bahi L, El-Yamine N. Preliminary survey of the structure and hydrogeology of the western Saiss Basin, Morocco, using electrical resistivity. J Afr Earth Sci. 2001;32(4):777-89. doi: 10.1016/S0899-5362(02)00054-4.
23. Qarqori K, Rouai M, Moreau F, Saracco G, Dauteuil O, Hermitte D, et al. Geoelectrical tomography investigating and modeling of fractures network around Bittit spring (Middle Atlas, Morocco). Int J Geophys. 2012;2012(1):489634. doi: 10.1155/2012/489634.
24. Kabbaj A, Combe M. Présentation du Domaine Atlasique. In: Editions du service géologique du Maroc, Ressources en eau du Maroc, domaine atlasique et sud atlasique. - Notes et mémoires du service géologique du Maroc. 1977;231:29-36.
25. ABHS - Anzar Conseil. Study of the groundwater modelling of the Fez-Meknes (Sais) plain. Technical Report, Mission I: Analysis andcritical studies in the plain by ABHS. 2005. P. 107.
26. Essahlaoui A. Contribution à la reconnaissance des formations aquifères dans le Bassin de Meknès-Fès (Maroc), Prospection géo-électrique, étude hydrogéologique et inventaire des

ressources en eau [dissertation]. Rabat, Maroc: Université Mohammed VI; 2000.
27. SHRD-Report of the Sebou Hydraulic Region Direction, 1990.
28. Harmouzi O, Riss J, Essahlaoui A, Marache A, Sirieix C. Interprétation de sondages électriques verticaux par combinaison de méthodes statistique, géostatistique et d'inversion: application au bassin de Saïss (Maroc). Afr Geosci Rev. 2009;16(2):119-40.
29. Aley T, Aley C, Elliott WR, Huntoon PW. Karst and cave resource significance assessment, Ketchikan area, Tongass National Forest, Alaska. Final Report, prepared for the Ketchikan Area of the Tongass National Forest. 1993.
30. Harmouzi O. Reconnaissance détaillée de la partie nord-est du Bassin de Saïss (MAROC): interprétation de sondages électriques verticaux par combinaison des méthodes statistique, géostatistique et d'inversion [dissertation]. Maroc: Université Moulay Ismail; 2010.
31. Ford DC, Williams PW. Karst Geomorphology and Hydrology. London: Unwin Hyman; 1989. p. 601.
32. Qarqori KH. Contribution to the study of the discontinuous and karstic reservoir of the Middle Atlasic Causses and its junction with the Saïs basin by remote sensing and geophysical imagery [dissertation]. Meknès, Morocco: Université Moulay Ismail; 2015.
33. Kirkland DW. National Cave and Karst Research Institute special paper 2: Role of hydrogen sulfide in the formation of cave and karst phenomena in the Guadalupe Mountains and Western Delaware Basin, New Mexico and Texas. Environmental Sustainability Books; 2014. https://scholarcommons.usf.edu/tlespub/3.
34. Bahaj T, Wartiti M, Zahraoui M, Essahlaoui A, Caboi R. Aspects of groundwater geochemistry from Middle Atlas and Saiss basin (Northern Morocco). In: Wanty RB, Seal RR, eds. Water–Rock Interaction. London: Taylor and Francis; 2004. p. 343-6.
35. White WB. Geomorphology and Hydrology of Karst Terrains. New York, NY: Oxford University Press; 1988. p. 464.
36. Didi S, Najine A. Application des méthodes géophysiques a l'étude structurale et dans l'identification des fissurées aquifères dans le plateau de Meknes, Maroc. Am J Innov Res Appl Sci. 2017;4(4):163-73.
37. Belkhiri A. Integrated water resources management, resource protection: Sebou Basin. Rev HTE. 2007;137:9-22.
38. Benaabidate L, Fryar AE. Controls on ground water chemistry in the central Couloir Sud Rifain, Morocco. Ground Water. 2010;48(2):306-19. doi: 10.1111/j.1745-6584.2008.00533.x.
39. Parkhurst DL, Appelo CA. User's guide to PHREEQC (Version 2): A computer program for speciation, batch-reaction, one-dimensional transport, and inverse geochemical calculations. US Geol Surv Water Resour Invest Rep. 1999;99-4259.
40. Simler R. Software "Diagrammes," Laboratoire d'Hydrologie d'Avignon, Université d'Avignon et pays du Vaucluse, France. 2012. Available from: http://www.lha.univ-avignon.fr.
41. Nour AM, Abderamane H, Idriss MY, Djekobe HA, Bouzed HB. Study of the physico-chemical and bacteriological quality of water intended for consumption in the town of Gagal, southwestern Chad. J Appl Nat Sci. 2023;15(3):908-16. doi: 10.31018/jans. v15i3.4560.
42. Rajmohan N, Masoud MHZ, Niyazi BA. Assessment of groundwater quality and associated health risk in the arid environment, Western Saudi Arabia. Environ Sci Pollut Res Int. 2021;28(8):9628-46. doi: 10.1007/s11356-020-11383-x.
43. Macioszczyk A, Dobrzyński D. Hydrogeochemia: strefy aktywnej wymiany wód podziemnych. Warszawa: Wydawnictwo Naukowe PWN; 2002. p. 448.
44. Dindane K, Bouchaou L, Hsissou Y, Boutaleb S. Caractérisation chimique et origine des eaux de la nappe libre du Souss amont (Bassin du Souss-Massa, Maroc). Afr Geosci Rev. 2007;14(3):329-35.
45. Fetterer F, Gineris D, Johnson C. Remote sensing aids in sea-ice analysis. Eos, Transactions American Geophysical Union. 1993;74(24):265-8. doi: 10.1029/93eo00380.
46. Thomas C, Orban P, Brouyère S. Mise en évidence des concentrations géochimiques de référence dans les nappes phréatiques tertiaires et du Socle en zone d'alimentation. Rapport final, Département d'Architecture, Géologie, Environnement & Constructions Université de Liège. Juillet 2019.
47. Michałowski T, Asuero AG. Thermodynamic modelling of dolomite behavior in aqueous media. Journal of Thermodynamics. 2012;2012(1):723052. doi: 10.1155/2012/723052.
48. Alayat H, LA Mouroux C. Caractérisation physico-chimique des eaux thermominerales des monts de la cheffia, (extrême N-E algérien) GEO-ECO-MARINA 13, Coastal Zone processes and management. Environmental Legislation. 2007; 75-84.
49. Stournaras G, Panag Oupoulos A, Sotiropoulou K. La signification hydrogéologique des conditions hydrochimiques et géomorphologiques d'un terrain gypseux, Les sources de Drymos (Grece occidentale), Annales de l'université de Provence, XVI. 1989.
50. Szymanska-Pulikowska A. Calcium and magnesium in underground waters around a communal waste dump. J Elementol. 2008;13(3):391-9.
51. Kumar SK, Rammohan V, Sahayam JD, Jeevanandam M. Assessment of groundwater quality and hydrogeochemistry of Manimuktha River basin, Tamil Nadu, India. Environ Monit Assess. 2009;159(1-4):341-51. doi: 10.1007/s10661-008-0633-7.
52. Subba Rao N. Factors controlling the salinity in groundwater in parts of Guntur district, Andhra Pradesh, India. Environ Monit Assess. 2008;138(1-3):327-41. doi: 10.1007/s10661-007-9801-4.
53. Matini L, Tathy C, Moutou JM. Seasonal groundwater quality variation in Brazzaville, Congo. Res J Chem Sci. 2012;2(1):7-14.
54. Audubert R. Les ions en solutions, P.U.F Paris. 1955; Tome 1, p.90.
55. Roques H. Fondements théoriques du traitement chimique des eaux. Paris: Technique et Documentation-Lavoisier; 1990.